Environ Monit Assess (2017) 189:170
DOI 10.1007/s10661-017-5879-5

Harmonization of forest disturbance datasets of the conterminous USA from 1986 to 2011

Christopher E. Soulard · William Acevedo · Warren B. Cohen · Zhiqiang Yang · Stephen V. Stehman · Janis L. Taylor

Received: 12 September 2016 / Accepted: 1 March 2017

Abstract Several spatial forest disturbance datasets exist for the conterminous USA. The major problem with forest disturbance mapping is that variability between map products leads to uncertainty regarding the actual rate of disturbance. In this article, harmonized maps were produced from multiple data sources (i.e., Global Forest Change, LANDFIRE Vegetation Disturbance, National Land Cover Database, Vegetation Change Tracker, and Web-Enabled Landsat Data). The harmonization process involved fitting common class ontologies and determining spatial congruency to produce forest disturbance maps for four time intervals (1986–1992, 1992–2001, 2001–2006, and 2006–2011). Pixels mapped as disturbed for two or more datasets were labeled as disturbed in the harmonized maps. The primary advantage gained by harmonization was improvement in commission error rates relative to the individual disturbance products. Disturbance omission errors were high for both harmonized and individual forest disturbance maps due to underlying limitations in mapping subtle disturbances with Landsat classification algorithms. To enhance the value of the harmonized disturbance products, we used fire perimeter maps to add information on the cause of disturbance.

Keywords Forest · Change detection · Harvest · Fire · Landsat · USA

Electronic supplementary material The online version of this article (doi:10.1007/s10661-017-5879-5) contains supplementary material, which is available to authorized users.

C. E. Soulard (✉)
Western Geographic Science Center, US Geological Survey, 345 Middlefield Road, MS-531, Menlo Park, CA 94025, USA
e-mail: csoulard@usgs.gov

W. Acevedo · J. L. Taylor
EROS Data Center, US Geological Survey, Sioux Falls, SD, USA

W. B. Cohen
PNW Research Station, US Department of Agriculture Forest Service, Corvallis, OR, USA

Z. Yang
Department of Forest Ecosyste and Society, Oregon State University, Corvallis, OR, USA

S. V. Stehman
Department of Forest and Natural Resources Management, State University of New York, Syracuse, NY, USA

Introduction

Effective spatial modeling of forest ecosystem processes relies on dependable maps with corresponding measures of uncertainty describing the spatio-temporal patterns of forest disturbance throughout time. Earth Observation Systems (EOS) provide quality, repeatable measurements appropriate for monitoring such vegetation change processes over time (Lunetta and Elvidge 1999). Until recently, slow computational processing times and the high cost of imagery limited the applicability of mid-resolution (i.e., Landsat 30 m) time series data suitable for short- and long-term vegetation trend analyses (Lunetta et al. 2006; Woodcock et al. 2008; Wulder et al. 2012). In recent years, the remote sensing

Published online: 18 March 2017

community has seen improvements in the temporal resolution of change detection efforts using Landsat imagery, with numerous advances in the mapping of forest change. Easy access to free Landsat imagery and advances in EOS processing (Hansen et al. 2014; Friedl et al. 2014) have effectively circumvented many of these prior constraints, and allowed greater use of the full 40+-year temporal record provided by the Landsat satellite program (Zhu and Woodcock 2014).

A wide array of forest disturbance data now exists (Fig. 1). Intercomparisons of forest disturbance products show considerable geospatial agreement, yet clear differences arise (Masek et al. 2013). Map products primarily vary based on the methods used to classify the imagery, specifically how forest and disturbance are defined and how sensitive each algorithm is to changes taking place on the ground (clear cuts, thinning, disease, fire, etc.). Different temporal revisit rates among mapping efforts also contribute to disagreement, with more disturbances typically mapped in those products where more Landsat images are used (i.e., temporally dense).

The major problem with forest disturbance mapping is that variability between map products leads to uncertainty regarding the actual rate of disturbance. Additionally, accuracy assessments and information on the proximate causes contributing to forest disturbance are only available for select data (Vogelmann et al. 2011; Wickham et al. 2013; Hansen et al. 2013). Forest disturbance maps are more informative to end users when classification accuracy is assessed (Zimmerman et al. 2013). Further, distinguishing between human-induced clearing and natural disturbances is a valuable enhancement to a disturbance product (Hansen et al. 2010). Combining a disturbance map that has undergone a rigorous accuracy assessment with information on the cause of disturbance (e.g., distinguishing fire from forest harvest) provides useful data for landscape modeling efforts (Olander et al. 2008) and carbon studies (Liski et al. 1998; Houghton 1999; Goward et al. 2008).

Multi-temporal data harmonization may be applied to highlight where forest disturbance data agree and reduce uncertainty regarding where disturbances occur. In its simplest form, harmonization involves a spatial join that merges attributes from one feature to another based on a shared spatial relationship. Harmonization has been used to reconcile differences between map products (Jung et al. 2006; See and Fritz 2006; Jansen 2006; Pérez-Hoyos et al. 2012) to make independent data interoperable or to make a resulting, synergistic product more useful by adding descriptive attributes. Other efforts have specifically harmonized forest and forest disturbance data to reduce errors and produce more reliable maps through convergence of evidence (Song et al. 2014; Schepaschenko et al. 2015). However, past forest harmonization efforts have typically used coarse resolution maps and a single map date. The harmonization method that we used is readily applicable at a national scale to generate wall-to-wall, spatially explicit maps representing forest disturbance. At the final stage, we implemented a simple decision rule to assign a pixel to the harmonized disturbed class by requiring two or more of the maps to have identified the pixel as forest disturbance. More complex rules that weight the input map products differently (see, for example, Drobne and Lisec 2009)

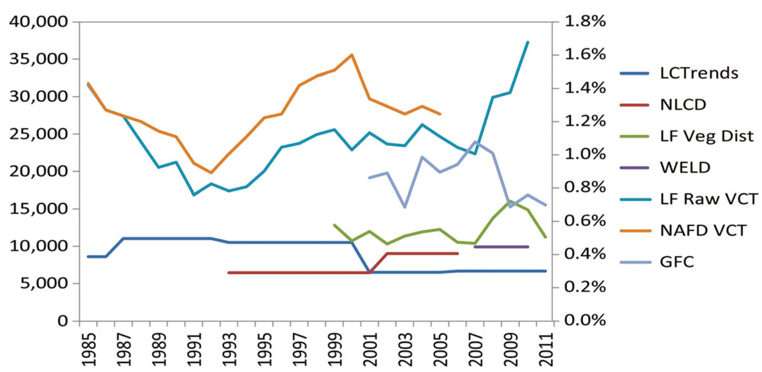

Fig 1 *Color*: annualized area of forest disturbance (km^2/year) and annualized disturbance as a percent of total forest (%) for CONUS across all readily accessible forest disturbance datasets created using Landsat imagery. Estimates from the USGS Land Cover Trends Project (Loveland et al. 2002; Soulard et al. 2014) and first version of North American Forest Dynamics (NAFD) VCT (Goward et al. 2008) are included for comparison (see Table 1 for description of products). Baseline forest area used to convert area disturbed to percent disturbed was obtained from 1987 CONUS forest estimates included in the 2010 USDA RPA (Oswalt et al. 2014)

could have been used, but we had no a priori basis for assigning such variable weights to the input products.

The primary goal of this study is to use a convergence of evidence approach to create improved maps of forest disturbance and to subject the harmonized maps as well as the input maps to a statistically rigorous accuracy assessment. An additional goal is to augment the disturbance map with information regarding the cause of the disturbance for pixels labeled as disturbed. The harmonization process is applied by intersecting national disturbance datasets at a moderate spatial resolution (30 m) using a pixel-based data fusion process. We create forest disturbance maps for conterminous USA (CONUS) across four time intervals, 1986–1992, 1992–2001, 2001–2006, and 2006–2011. These time intervals were selected to allow inclusion of NLCD map products to increase the quantity of forest disturbance data incorporated into the harmonization process. The harmonization process indicates where disturbance products are congruent by identifying pixels mapped as disturbed by more than one product. Once the initial harmonization is complete, we intersect fire data with the harmonized disturbance maps to distinguish disturbance attributable to fire from other causes of disturbance. Finally, an accuracy assessment is performed on the harmonized maps and selected individual maps to evaluate how well current mapping processes capture forest disturbance. Disturbance magnitude determined from reference data collected by the US Forest Service is used to identify the types of forest disturbance currently omitted from maps.

Data

The number and variety of maps representing forest disturbance in the CONUS is rapidly growing (Table 1). Landsat imagery has proven to be effective in evaluating forest characteristics over time (Goetz et al. 2006; Fensholt et al. 2009), providing a mechanism to identify abrupt forest changes (Moisen and Frescino 2002). Five readily accessible forest disturbance wall-to-wall CONUS products derived from Landsat were used in this study: Global Forest Change (GFC) (Hansen et al. 2013), LANDFIRE Vegetation Disturbance (LF) (Rollins 2009; Vogelmann et al. 2011; Nelson et al. 2013), National Land Cover Dataset (NLCD) (Vogelmann et al. 2001; Homer et al. 2004; Xian et al. 2009; Jin et al. 2013), data delivered to the LANDFIRE program by the North American Carbon Program (NACP) using the Vegetation Change Tracker (VCT) process (hereafter referred to as LF Raw VCT) (Huang et al. 2010), and Web-Enabled Landsat Data (WELD) (Roy et al. 2010; Hansen et al. 2011). Monitoring Trends in Burn Severity (MTBS) (Finco et al. 2012) was used to identify forest disturbance due to fire.

GFC data include global tree cover extent, loss, and gain for the period 2000–2012 at a 30-m spatial resolution based on Landsat satellite imagery (Hansen et al. 2013). Tree cover losses are tracked in every Landsat scene, yet spatially explicit tree cover loss maps summarize change annually. GFC does not assign causality to change pixels. LF data include forest disturbance for CONUS for the period 1999–2012 at a 30-m spatial resolution based on Landsat imagery, local agency-derived disturbance polygons, and other ancillary data. Spatially explicit maps are composited annually and classify disturbance causality (Vogelmann et al. 2011). NLCD data include land-use/land-cover (LULC) transitions for CONUS for three periods spanning 1992–2011 at a 30-m spatial resolution based on Landsat (Vogelmann et al. 2001; Homer et al. 2004; Fry et al. 2009; Xian et al. 2009; Jin et al. 2013). Spatially explicit maps representing transitions from forest land-cover classes and the woody wetland class are created for 1992–2001, 2001–2006, and 2006–2011 to measure forest disturbance. LF Raw VCT data include persistent non-forest, persistent forest, and forest disturbance for CONUS for the period 1985–2010 at a 30-m spatial resolution based on Landsat satellite imagery (Huang et al. 2010). Spatially explicit maps of forest disturbance change are compiled annually. LF Raw VCT marks first and last disturbance dates but does not assign causality to forest change pixels. WELD data include tree cover loss for CONUS and Alaska for the period 2006–2010 at a 30-m spatial resolution based on Landsat image composites. WELD maps tree cover loss annually and aggregates losses over a 5-year window but does not assign causality to change pixels (Roy et al. 2010; Hansen et al. 2011). MTBS data include CONUS fire severity at a 30-m spatial resolution and vector fire perimeters for the period 1984–present. Although fire data are compiled continuously based on Landsat, and by local agencies using a suite of different techniques, data files are summarized annually (Finco et al. 2012). All fires greater than 1000 acres in the western USA and 500 acres in the eastern USA are mapped by MTBS. MTBS may be used to establish a causal identifier for forest fire disturbances.

Table 1 Summary of forest disturbance and fire datasets, including minimum mapping unit (MMU), the years used in this analysis, source input data, the amount of Landsat images incorporated into the disturbance mapping, and the class definition used as a proxy for forest disturbance

Dataset	MMU	Years used	Source	No. of Landsat images used	Class definition
Global Forest Change (GFC)	30 m	2000–2012	Landsat	Near continuous Landsat time series	The term forest refers to tree cover and not land use. Trees are defined as vegetation taller than 5 m in height. Forest loss is defined as a stand-replacement disturbance or the complete removal of tree cover canopy at the Landsat pixel scale. Gain is defined as the inverse of loss, or a non-forest to forest change (Hansen et al. 2013). For this effort, annual losses were aggregated for each time interval.
LANDFIRE Vegetation Disturbance (LF)	30 m[a]	1999–2012	Landsat and cooperator-provided data	Integrated Landsat composites using bi-annual images optimized for change detection	LANDFIRE vegetation disturbance is primarily focused on forest cover, which is defined by NatureServe's Ecological Systems classification. Forest cover change processes are flagged annually by cooperator-provided data and by evaluating vegetation in a Landsat time series. A significant deviation from the prior year (increase in the integrated forest *z*-score) indicates the occurrence of a disturbance in that year. Ancillary data contribute to the assignment of proximate cause (Vogelmann et al. 2011). For this effort, all disturbance classes were aggregated to a single class and annual disturbances were aggregated for each time interval.
LANDFIRE Raw Vegetation Change Tracker (LF Raw VCT)	60 m	1985–2010	Landsat	Landsat time series stacks using one Landsat image per year	VCT is an automated algorithm that uses Landsat time series stacks to map changes in forest cover based on the spectral indexes indicating the likelihood of each pixel being a forest pixel. Annual maps classify pixels showing "first" and "last" disturbances that occurred in that year. For this effort, annual maps of "last" disturbance were aggregated for each time interval.
National Land Cover Data (NLCD)	30 m[a]	1992–2001; Retro 1992–2001; 2001–2006; 2006–2011	Landsat	Integrated Landsat composites using bi-annual images optimized for change detection	Forest is defined as areas dominated by trees generally greater than 5 m tall, and greater than 20% of total vegetation cover (Vogelmann et al. 2001; Homer et al. 2004). For this effort, evergreen forest, deciduous forest, mixed forest, and woody wetlands were considered the "from" class and barren, grass, shrubland, and herbaceous wetland were considered the "to" class to represent forest disturbances between two NLCD map dates.

Table 1 (continued)

Dataset	MMU	Years used	Source	No. of Landsat images used	Class definition
Web-Enabled Data (WELD)	30 m	2006–2010	Landsat	Near continuous Landsat time series	A decision tree classification algorithm was used with expert-derived training data to identify forest cover loss and bare ground gain (Hansen et al. 2011, 2014). For this effort, the "LCLUC_TREE_COVER_LOSS" product that identifies tree loss (yes or no) over a 5-year period (2006–2010) was used.
Monitoring Trends in Burn Severity (MTBS)	30 m	1984–2012	Landsat and cooperator-provided data	Landsat applied to identify fire perimeters and severity in post-fire imagery	Fire perimeter and severity for moderate-to-large fires were flagged annually by cooperator-provided data, on-screen interpretation, and by evaluating Normalized Burn Ratio products derived using Landsat images and Landsat time series (Finco et al. 2012). For this effort, annual fire maps were aggregated for each time interval.

Only two datasets have national accuracy assessments published (GFC and NLCD 2001–2006), and one dataset includes causal classes (LF)

[a] Some filtering to remove single pixels

Methods

Harmonization of land-use or land-cover data is implemented using simple image processing functions that create a composite image of multiple raster input datasets. The composite is created by combining multiple datasets and assigning an output value to each unique combination of input datasets. The resulting composite requires reviewing the resulting classes and determining an appropriate cutoff for the number of datasets required to be in agreement for a pixel to be considered classified (i.e., harmonized) for the land use or land cover in question. Potential outcomes can range from all input datasets labeling a pixel as a specific land cover to just one dataset having mapped a pixel as the cover in question. Pixels where only one input dataset maps the land-cover or land-use type in question often reflect spectral classification confusion and are likely candidates for exclusion. The methodology involves recoding the composite datasets into binary land-cover/land-use map files using the selected dataset agreement threshold. To facilitate overlaying of independent geospatial data, all layers are co-registered to the same projection and spatial resolution. Temporal differences between inputs data sources are reconciled by grouping maps into common temporal intervals. To create a common classification legend across datasets, we fit class ontologies by aggregating classes to increase consistency between products (Jung et al. 2006; Jansen 2006). Below, we explain how map harmonization is specifically applied using forest disturbance data.

Harmonization of forest disturbance datasets The forest disturbance layers included in the harmonization process are listed in Table 2. Initially, the forest disturbance datasets acquired for the harmonization were co-registered to the same projection (Albers Conical Equal Area) and spatial resolution (30 m), recoded to binary forest disturbance datasets, and separated into one of four temporal intervals (1986–1992, 1992–2001, 2001–2006, and 2006–2011). GFC and WELD data required an additional mosaicking step prior to re-projection. Forest disturbance categories were generalized for LF by aggregating all forest disturbance classes into a single class, and for the NLCD and NLCD Retrofit products by collapsing all forest cover and woody wetland transitions to barren, grassland, and shrubland into a forest disturbance class (referred to as "forest cover disturbance" in Table 2).

Table 2 National datasets included in harmonization process

Time period	Datasets used in harmonization
1986–1992	NLCD 1992 transitional, grassland, and shrubland classes
	LF Raw VCT 1987–1992 forest disturbance
	NLCD Retrofit grassland and shrubland classes
1992–2001	NLCD 1992–2001 forest cover disturbance
	NLCD Retrofit 1992–2001 forest to grassland/shrubland and forest to barren
	LF Raw VCT 1993–2001 forest disturbance
	LF Veg Dist 1999–2001
2001–2006	NLCD 2001–2006 forest cover disturbance
	LF Raw VCT 2002–2006 forest disturbance
	LF Veg Dist 2002–2006
	GFC 2002–2006 tree cover loss
2006–2011	LF Raw VCT 2007–2010 forest disturbance
	LF Veg Dist 2007–2010
	WELD 2006–2010 tree cover loss
	GFC 2006–2011 tree cover loss
	NLCD 2006–2011 forest cover disturbance

A composite of the various forest disturbance input datasets was processed by combining multiple raster datasets, resulting in pixels with output values determined by the input products for which that pixel was labeled as disturbed forest. The next step was to determine an appropriate threshold for the number of datasets required to be in agreement for a pixel to be classified as forest disturbance in the harmonized map. Thresholds considered ranged from all input datasets labeling a pixel as forest disturbance to only one dataset having mapped a pixel as forest disturbance. The pixels where a single input dataset mapped a forest disturbance rarely formed cohesive patches across the landscape and actual disturbances were often visually undetectable in reference orthoimagery, leading us to exclude these pixels due to the lack of corroborating evidence. Further visual inspection of the maps produced from different thresholds along with qualitative comparisons to imagery led to a final decision specifying that pixels with two or more datasets in agreement of forest disturbance would be included in the harmonized map. Clearly, the harmonized map for a particular time interval is dependent on number of input layers and consequently our ability to compare disturbance rates across different time intervals is diminished. However, given that the primary objective was to produce the highest quality harmonized product for each time interval, we chose to take advantage of the greater number of disturbance products available for the more recent time intervals. The next step in the mapping protocol involved recoding the composite datasets into binary images of forest disturbance using the specified rule for assigning a pixel to the disturbed class in the harmonized products.

To create the harmonized 1986–1992 forest disturbance dataset, LF Raw VCT forest disturbance data delivered to the LANDFIRE program was harmonized with a surrogate forest disturbance class in the 1992 NLCD dataset (defined by the grassland/herbaceous, shrubland, and transitional classes), and a surrogate forest disturbance class in the 1992 NLCD Retrofit dataset defined by the grassland/shrub class (Table 2). The transitional class was used by NLCD to map sparse vegetative cover dynamically changing from one land cover to another because of land-use activities including forest clear cuts, a transition phase between forest and agricultural land, the temporary clearing of vegetation, and changes due to natural causes. Grassland and shrubland classes do not directly reflect forest change, yet were included as possible corroborating evidence in the event that forested lands pre-dated the 1992 NLCD map(s).

To harmonize data for the following interval (1992–2001), 1993–2001 LF Raw VCT vegetation disturbance data were harmonized with 1992–2001 NLCD forest disturbance, 1992–2001 NLCD Retrofit forest disturbance, and 1999–2001 LF aggregated forest disturbance (Table 2). To create the harmonized 2001–2006 forest disturbance dataset, 2002–2006 LF Raw VCT forest disturbance was harmonized with 2002–2006 LF aggregated forest disturbance, 2002–2006 GFC tree cover loss, and 2001–2006 NLCD forest disturbance. To create the harmonized 2006–2011 forest disturbance dataset, 2007–2010 LF Raw VCT forest disturbance was harmonized with a 2007–2011 LF aggregated forest disturbance, 2007–2011 GFC tree cover loss, 2006–2010 WELD tree cover loss, and 2006–2011 NLCD forest disturbance.

We visually assessed all resulting products against aerial imagery from regions of the USA with a long history of forest harvest. In two of the time intervals, our qualitative observations led to a modification in the harmonization method to include or exclude specific combinations of input datasets to achieve stronger correspondence to disturbances observed on the ground. In 2006–2011, we excluded select combinations of input data because these pixels did not align with forest disturbances in aerial photography. For example, a large collection of pixels along the coast of Oregon were mapped as disturbed by LF and LF Raw VCT but were deleted because these areas did not correspond to real changes. In the second case (1986–1992), where input data were sparse, we identified some actual areas of disturbance in LF Raw VCT that were omitted during the harmonization, including many clear-cut parcels along the coast in northern California. In the latter case, we added in large patches (above 4 ha) contained in the LF Raw VCT product to better represent the true amount of disturbance. The modifications are clearly indicated in Table 3.

Adding Causal Information to Harmonized Maps The general harmonized maps indicate if and when a forest disturbance occurred but do not assign the proximate cause of the disturbances to pixels in each map. In the second processing step, we intersected the harmonized disturbance maps with MTBS fire perimeter boundaries for the corresponding time intervals resulting in datasets with forest disturbance due to fire differentiated from forest disturbance due to other reasons (i.e., harvesting, insect damage, tornadoes, etc.). MTBS fires in other land-cover types (grassland, shrubland, etc.) were ignored during this stage. The process of overlaying MTBS fire perimeters on top of harmonized forest disturbance maps to identify forested areas disturbed by fire was repeated for each interval (1986–1992, 1992–2001, 2001–2006, and 2006–2011).

Illustrative examples of forest disturbance To provide an illustration of the temporal and spatial patterns of disturbance, we describe detailed results for two heavily forested areas, the Pacific Northwest and the Southeastern USA. The mean patch size for each class was summarized by time interval for the Pacific Northwest and the Southeastern USA. While final maps retain a 30-m MMU consistent with the majority of input data, we used established procedures consistent with other forest change efforts to form more cohesive patches and to assess and illustrate patch area regionally in each time interval (Woodcock et al. 2001; Cohen et al. 2002). The map products were filtered using a 3 × 3 nearest-neighbor approach (Cohen et al. 2002), patches were converted to vectors, and small patches were removed (less than 2 ha). The Pacific Northwest region includes 11 EPA Level II Ecoregions (Omernik 1987) (1, Coast Range; 2, Puget Lowlands; 3, Willamette Valley; 4, Cascades; 5, Sierra Nevada; 9, Eastern Cascades; 10, Columbia Plateau; 11, Blue Mountains; 15, Northern Rockies; 77, Middle Rockies; and 78, Klamath) and the Southeastern USA region includes 12 ecoregions (35, South Central Plains; 36, Ouachita Mountains; 45, Piedmont; 63, Middle Atlantic Coastal Plain; 65, Southestern Plains; 66, Blue Ridge Mountains; 67, Ridge and Valley; 68, Southwestern Appalachians; 69, Central Appalachians; 73, Mississippi Alluvial Plain; 75, Southern Coastal Plain; and 76, Southern Florida Coastal Plain).

Accuracy assessment

We performed an accuracy assessment to determine the relative improvement in forest disturbance mapping between harmonized maps and stand-alone maps for all four mapping intervals. The accuracy assessment was performed by comparing maps from each interval against sample reference plots selected as part of the US Forest Service-led forest dynamics characterization study using the TimeSync Landsat time series visualization and change data collection tool (Cohen et al. 2016). The two-stage stratified cluster design initially delineated five regional strata across CONUS that combined different ecoregions sharing similar forest types. A fixed hexagonal grid of 442 Thiessen Scene Areas (TSA) was draped over CONUS and the number of random TSAs to sample was chosen for each stratum based on the proportion of forest (Kennedy et al. 2010). A stratified random sample of 180 TSAs was selected, and a simple random sample of 40 Landsat plots (30 m pixels) was selected within each TSA, leading to a sample size of 7200 reference plots. Reference plots were interpreted using the TimeSync response design, which evaluated forest disturbance type, duration, and magnitude from 1985 to 2012 (Cohen et al. 2010). TimeSync interpretations were aided by visual interpretation of high-resolution images in Google Earth. Forest inventory data were used in visual interpretations where possible.

The accuracy of the forest disturbance products was summarized by estimating a confusion matrix and associated parameters such as overall accuracy and omission and commission error rates following good practice recommendations for accuracy assessment (Olofsson et al. 2014). The accuracy estimates were produced using the SURVEYMEANS procedure of the Statistical Analysis Software (SAS) (SAS/STAT version 9.3). Each TSA cluster (denoted by the subscript i) belonged to one of the five regional strata. A ratio

Table 3 Outcome of the forest disturbance harmonization summarized by the number of pixels for which all datasets in the listed time interval labeled the pixel as disturbed and the final decision to include (*Y*) or exclude (*N*) each subset in the final (composite) harmonized product

Pixel count	No. of datasets	Description of datasets	Included
1986–1992			
4,620,148	3	LF Raw VCT and NLCD transitional and Retro grass/shrub	Y
11,013,715	2	LF Raw VCT and NLCD transitional	Y
3,710,700	2	LF Raw VCT and Retro grass/shrub and NLCD grass/shrub	Y
11,600,818	2	NLCD transitional and Retro grass/shrub	Y
4,486,782	2	LF Raw VCT and NLCD grass/shrub	Y
13,993,434	2	LF Raw VCT and Retro grass/shrub	Y
46,308,184	1	NLCD transitional only	N
2,631,200,130	1	NLCD grass/shrub and Retro grass/shrub (supporting data only)	N
78,515,608	1	LF Raw VCT only	Y[a]
252,217,873	1	NLCD grass/shrub only	N
476,870,365	1	Retro grass/shrub only	N
1992–2001			
12,303,507	4	LF and Retro forest dist and NLCD forest dist and LF Raw VCT	Y
13,661,974	3	LF and NLCD forest dist and LF Raw VCT	Y
440,320	3	LF and Retro forest dist and LF Raw VCT	Y
1,333,011	3	LF and Retro forest dist and NLCD forest dist	Y
22,313,868	3	Retro forest dist and NLCD forest dist and LF Raw VCT	Y
14,517,259	2	LF and LF Raw VCT	Y
6,721,381	2	LF and NLCD forest dist	Y
405,420	2	LF and Retro forest dist	Y
58,208,177	2	NLCD forest dist and LF Raw VCT	Y
1,417,314	2	Retro forest dist and LF Raw VCT	Y
15,798,188	2	Retro forest dist and NLCD forest dist	Y
10,139,379	1	LF only	N
81,872,158	1	LF Raw VCT only	N
367,723,324	1	NLCD forest dist only	N
10,842,672	1	Retro forest dist only	N
2001–2006			
20,014,990	4	GFC and LF and LF Raw VCT and NLCD	Y
2,429,743	3	LF and LF Raw VCT and NLCD	Y
6,077,550	3	GFC and LF Raw VCT and NLCD	Y
626,356	3	GFC and LF and NLCD	Y
21,214,853	3	GFC and LF and LF Raw VCT	Y
1,890,325	2	LF Raw VCT and NLCD	Y
310,135	2	LF and NLCD	Y
10,270,859	2	LF and LF Raw VCT	Y
5,184,346	2	GFC and NLCD	Y
16,386,783	2	GFC and LF Raw VCT	Y
1,469,036	2	GFC and LF	Y
14,274,750	1	NLCD only	N
33,693,479	1	LF Raw VCT only	N

Table 3 (continued)

Pixel count	No. of datasets	Description of datasets	Included
10,300,344	1	LF only	N
29,805,203	1	GFC only	N
2006–2011			
19,044,980	5	WELD and LF Raw VCT and LF and GFC and NLCD	Y
6,988,814	4	GFC and LF and WELD and LF Raw VCT	Y
1,498,124	4	WELD and LF Raw VCT and LF and NLCD	Y
2,675,939	4	WELD and LF Raw VCT and GFC and NLCD	Y
3,016,365	4	WELD and LF and GFC and NLCD	Y
5,037,136	4	LF Raw VCT and LF and GFC and NLCD	Y
1,718,469	3	LF and WELD and LF Raw VCT	Y
2,336,832	3	GFC and WELD and LF Raw VCT	Y
3,554,503	3	GFC and LF and WELD	Y
6,672,230	3	GFC and LF and LF Raw VCT	Y
707,153	3	WELD and LF Raw VCT and NLCD	Y
830,684	3	WELD and LF and NLCD	Y
1,886,199	3	LF Raw VCT and LF and NLCD	Y
1,446,003	3	WELD and GFC and NLCD	Y
1,664,820	3	LF Raw VCT and GFC and NLCD	Y
5,268,471	3	LF and GFC and NLCD	Y
5,515,703	2	WELD and LF Raw VCT	N[b]
1,199,260	2	LF and WELD	N[b]
8,327,447	2	LF and LF Raw VCT	N[b]
1,706,240	2	GFC and WELD	Y
6,794,714	2	GFC and LF Raw VCT	N[b]
9,700,715	2	GFC and LF	Y
1,123,252	2	WELD and NLCD	N[b]
1,680,776	2	LF Raw VCT and NLCD	N[b]
3,282,248	2	LF and NLCD	N[b]
2,878,215	2	GFC and NLCD	Y
7,815,951	1	WELD only	N
50,047,164	1	LF Raw VCT only	N
104,358,182	1	LF only	N
21,794,563	1	GFC only	N
13,616,155	1	NLCD only	N

[a] 36,423,361 pixels included based on comparison with aerial photos

[b] Pixels excluded based on comparison with aerial photos

estimator was used to estimate the accuracy parameters (SAS/STAT version 9.3),

$$\hat{R} = \frac{\sum_{h=1}^{5}\sum_{i=1}^{n_h}\sum_{j=1}^{40} w_{hij}y_{hij}}{\sum_{h=1}^{5}\sum_{i=1}^{n_h}\sum_{j=1}^{40} w_{hij}x_{hij}} \quad (1)$$

where h was the stratum index (h = 1, ..., 5), i was the index of the TSA within stratum h for the sample of n_h TSAs selected from stratum h ($i = 1, 2, \ldots, n_h$), and j was the index of the pixel within TSA i of stratum h (j = 1, …, 40). The observations x_{hij} and y_{hij} were defined to yield the accuracy parameter of interest (see explanation below), and w_{hij} was the estimation weight (i.e., inverse of the inclusion probability) for sample pixel j in TSA i of stratum h. The inclusion probability of a TSA from stratum h was n_h/N_h where n_h and N_h were the number of TSAs in the sample and population for stratum h. The inclusion probability for each pixel within TSA i of stratum h, conditional on this TSA being selected in the first-stage sample, was $40/M_{hi}$, where M_{hi} is the number of pixels within this TSA. The inclusion probability for a pixel over both stages of sampling was then the product of the first-stage and conditional second-stage inclusion probability,

$$\frac{n_h}{N_h}\frac{40}{M_{hi}} \tag{2}$$

To estimate overall accuracy, we defined $y_{hij} = 1$ if pixel j of TSA i of stratum h was correctly classified ($y_{hij} = 0$ otherwise) and defined $x_{hij} = 1$ for every sampled pixel. To estimate commission error of disturbed forest, we defined $y_{hij} = 1$ if sample pixel j of TSA i in stratum h was mapped as disturbed but incorrectly classified as not disturbed (otherwise $y_{hij} = 0$), and defined $x_{hij} = 1$ if the sample pixel was mapped as disturbed (otherwise $x_{hij} = 0$). Lastly, to estimate omission error, we defined $y_{hij} = 1$ if pixel i had TimeSync (reference) class disturbed forest and was incorrectly classified as not disturbed forest (otherwise $y_{hij} = 0$) and defined $x_{hij} = 1$ if pixel i had reference class of disturbed forest. For each accuracy measure, the appropriate values of x_{hij} and y_{hij} were inserted into Eq. (1).

The variance estimator for the accuracy estimates produced using Eq. (1) was based on a Taylor series approximation (Särndal et al. 1992):

$$\hat{V}\left(\hat{R}\right) = \sum_{h=1}^{5}\hat{V}_h\left(\hat{R}\right) = \sum_{h=1}^{5}\frac{n_h\left(1-\frac{n_h}{N_h}\right)}{(n_h-1)}\sum_{i=1}^{n_h}\left(g_{hi}-\overline{g}_h\right)^2 \tag{3}$$

where

$$g_{hi} = \frac{\sum_{j=1}^{40} w_{hij}\left(y_{hij}-x_{hij}\hat{R}\right)}{\sum_{h=1}^{5}\sum_{i=1}^{n_h}\sum_{j=1}^{40} w_{hij}x_{hij}} \tag{4}$$

and

$$\overline{g}_h = \left(\sum_{i=1}^{n_h} g_{hi}\right)/n_h \tag{5}$$

The standard error of the estimated accuracy measure was the square root of the estimated variance provided by Eq. (3).

The TimeSync information for the sample of reference plots was also used to assess the magnitude of the forest disturbances being captured by the harmonization process as well as the magnitude of forest disturbances being omitted. The intensity of disturbance in the reference plots was calculated as the relative amount of reflectance change associated with the disturbance (Cohen et al. 2016). The relative change in the normalized burn ratio (NBR) was calculated for each reference plot and assigned a category based on magnitude: high (>66% relative change), medium (between 33 and 66% relative change), and low (<33% relative change) (Kennedy et al. 2012).

Results

Convergence between input datasets

Table 3 presents the final results of the forest disturbance harmonization. Results indicate convergence (as quantified by the number of input datasets agreeing that the pixel was disturbed) increased between input datasets in each subsequent time interval. For 1986–1992, there were many pixels where the minimum convergence threshold was met, but only 5% of these pixels selected for the final harmonized map matched between all three input datasets. For 1992–2001, three or more datasets agreed that the pixel was disturbed for 34% of the pixels mapped as disturbed forest in the final harmonized map. In the last two time periods (2000–2006 and 2006–2011), three or more datasets agreed that the pixel was disturbed 59 and 82% of the pixels mapped as disturbed in the harmonized maps of these time periods. Moreover, 24% of the pixels selected in the 2006–2011 forest disturbance map matched between all five input datasets, suggesting increasing convergence between products. Over the same interval, the amount of forest disturbance with no convergence was relatively low for each input product. The land area mapped as disturbed by single products ranged from 12,000 km^2 (NLCD) to 94,000 km^2 (LF).

Description of general temporal and spatial patterns of harmonized maps

Average annual rates of forest disturbance per time period ranged from 13,072 km^2/year for 1986–1992 to 15,667 km^2/year for 2001–2006, equivalent to approximately 0.5–0.6% forest disturbed/year. Comparison of the overall harmonized disturbance rates with those of the individual constituent products showed that the harmonized rates were lower than those of LF Raw VCT, LANDFIRE, and GFC but higher than the rates of Land Cover Trends and NLCD (Fig. 1). Comparatively, the average annual rate of forest disturbance mapped by LF Raw VCT ranged from 22,919 km^2/year for 1986–1992 to 25,636 km^2/year for 2001–2006, nearly 10,000 km^2/year more than the harmonized maps. Similarly, total forest disturbance in harmonized maps was far lower compared with LF Raw VCT between 1986 and 2011, with approximately 366,500 and 569,800 km^2 disturbed across CONUS for each respective product (Fig. 2; disturbance raster data are included as supplementary material). LF Raw VCT data were used in the quantitative comparison because these data represent the only maps spanning the entire study period.

Figure 3 illustrates examples of the detailed spatial patterns of disturbance in the Pacific Northwest and Southeastern USA. In terms of other broad descriptive features of the harmonized maps, a higher percentage of the overall area in the Southeastern USA was disturbed in each interval, although forest fires represented a larger portion of the forest disturbance in the West. While the harvest/other class incorporated natural and anthropogenic conversions of variable patch shape and size, the class was largely composed of harvest with clearly defined patch shapes and size. The trend in mean patch size over time indicated that harvest size increased slightly over time in the Pacific Northwest and the Southeastern USA (Fig. 4). Average forest fire patch area was larger than average harvest patch area. Patch size was highly variable between the Pacific Northwest and the Southeastern USA. The forest fire patch area was 55 to 304% larger in the Pacific Northwest, depending on the interval. The larger fire area in the West is well established, although we acknowledge that the use of MTBS as a proxy for fire may bias patch size regionally due to the different minimal area requirements between the western (1000-acre minimum, approx. 405 ha) and eastern USA (500-acre minimum, approx. 202 ha).

Accuracy and disturbance magnitude

The overall accuracy was high in all time intervals for both the harmonized data and the individual contributor maps, as would be expected given the high proportion of area that was not disturbed. This was most evident for 1986–1992 where the amount of disturbance was lowest and the overall accuracy was highest. The lowest overall accuracy occurred for 1992–2001. The differences in mapping accuracy between the early and late intervals

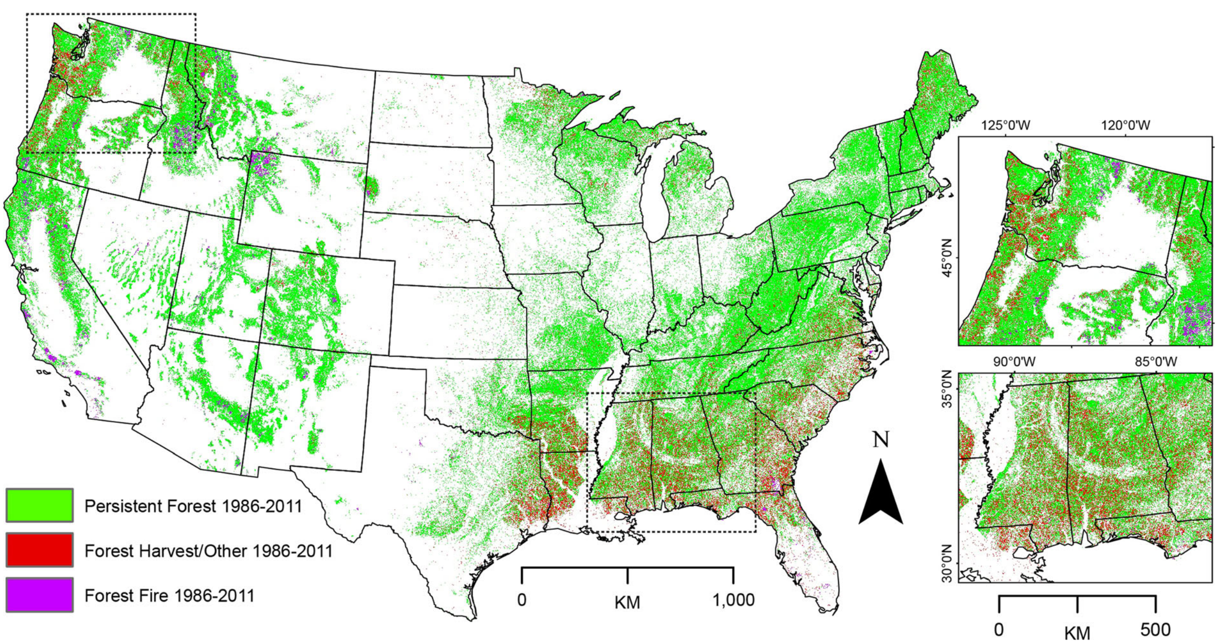

Fig. 2 *Color*: forest disturbances and persistent forest spanning 1986–2011. All four final harmonized maps (1986–1992, 1992–2001, 2001–2006, and 2006–2011) are aggregated, with forest harvest/other pixels displayed in *red* and forest fire pixels displayed as *magenta* (disturbance raster data are included as Supplementary material)

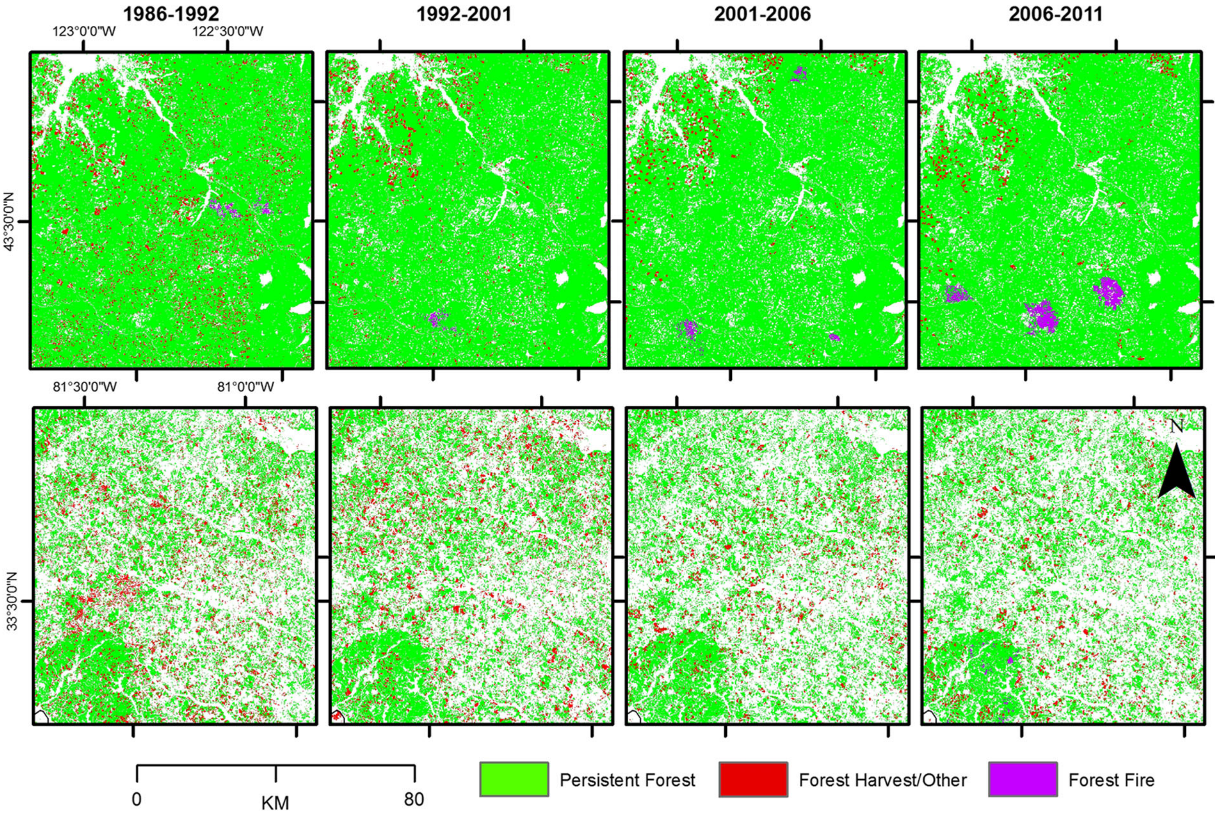

Fig. 3 *Color*: *top four panels* illustrate mapped forest disturbance patterns by interval in the Pacific Northwest (Oregon, USA). *Bottom four panels* illustrate forest disturbance patterns by interval in the Southeastern USA (South Carolina, USA)

may be indicative of the algorithms used to generate input products available for 1986–1992 and 1992–2001, particularly the LF Raw VCT data. The LF Raw VCT data served as a major input in the harmonization of forest disturbance throughout the 1980s and 1990s (Table 3) and commonly mapped more total disturbance compared with other products. As a stand-alone product, differences in the LF Raw VCT algorithm led to less omission error but higher commission errors. However, using LF Raw VCT in conjunction with other data results in a harmonized product with dramatically lower commission error compared with LF Raw VCT in the first two time intervals.

Harmonized disturbance maps had very high omission errors in all time intervals (Table 4). The omission errors of several other conventional datasets (GFC, LANDFIRE, and LF Raw VCT) were also quite high; however, it was common that at least one of the

Fig. 4 *Grayscale*: mean patch area for the Pacific Northwest and the Southeastern USA show that mapped harvest patch size did not differ substantially by region. However, mapped forest fire patches were consistently larger in the Pacific Northwest

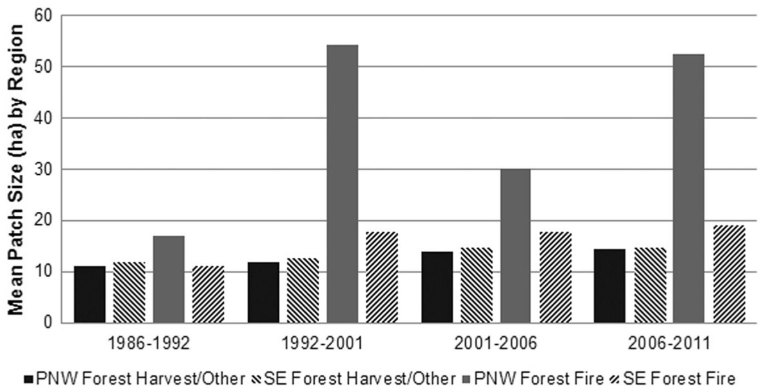

Table 4 Accuracy assessment of harmonized map and best single input map for each time interval

	Disturbed	Non-disturbed	Area total	Commission
A1) 1986–1992 harmonized				
Disturbed	0.9	0.2	1.1	20.2 (4.9)
Non-disturbed	2.8	96.2	98.9	2.8 (0.3)
Area total	3.6	96.4	100.0	
Omission	76.1 (2.9)	0.2 (0.1)		Overall 97.0 (0.3)
A2) 1986–1992 LF Raw VCT				
Disturbed	1.1	0.5	1.6	30.8 (5.0)
Non-disturbed	2.5	95.9	98.4	2.6 (0.2)
Area total	3.6	96.4	100.0	
Omission	69.8 (3.0)	0.5 (0.1)		Overall 97.0 (0.3)
B1) 1992–2001 harmonized				
Disturbed	1.2	0.3	1.5	18.5 (4.1)
Non-disturbed	4.8	93.7	98.5	4.9 (0.4)
Area total	6.1	93.9	100.0	
Omission	79.9 (1.7)	0.3 (0.1)		Overall 94.9 (0.4)
B2) 1992–2001 LF Raw VCT				
Disturbed	2.1	4.4	6.5	67.5 (2.7)
Non-disturbed	3.9	89.5	93.5	4.2 (0.4)
Area total	6.1	93.9	100.0	
Omission	65.1 (2.4)	4.7 (0.3)		Overall 91.6 (0.5)
C1) 2001–2006 harmonized				
Disturbed	0.9	0.1	1.0	9.3 (3.3)
Non-disturbed	3.8	95.2	99.0	3.9 (0.3)
Area total	4.7	95.3	100.0	
Omission	80.9 (2.3)	0.1 (0.0)		Overall 96.1 (0.3)
C2) 2001–2006 LANDFIRE				
Disturbed	1.1	0.1	1.3	11.7 (4.3)
Non-disturbed	3.6	95.1	98.7	3.6 (0.3)
Area total	4.7	95.3	100.0	
Omission	76.3 (2.4)	0.2 (0.1)		Overall 96.3 (0.3)
D1) 2006–2011 harmonized				
Disturbed	0.9	0.1	1.0	11.0 (5.8)
Non-disturbed	3.3	95.6	99.0	3.4 (0.3)
Area total	4.3	95.7	100.0	
Omission	78.2 (2.3)	0.1 (0.0)		Overall 96.6 (0.3)
D2) 2006–2011 GFC				
Disturbed	1.1	0.1	1.2	10.5 (3.3)
Non-disturbed	3.2	95.6	98.8	3.2 (0.3)
Area total	4.3	95.7	100.0	
Omission	74.8 (2.4)	0.1 (0.0)		Overall 96.7 (0.3)

Cell entries of confusion matrices are percent area of the conterminous USA. All accuracy and error rates are also expressed in percent (%). Overall accuracy is shown in bold. Standard errors are shown in parentheses

individual input maps had slightly lower omission errors than the harmonized maps. High omission errors suggest that many forest disturbances were missed across mapping efforts relative to the TimeSync reference classification. The TimeSync protocol is highly effective at detecting low magnitude forest disturbance, and this contributed to overall disturbance rates identified by the reference classification being three to six times greater than any of the input spatial datasets. Therefore, all comparisons included here suggest that disturbance was grossly underestimated by both the harmonized and input maps. We further describe the magnitude of omitted disturbances at the end of this section.

The harmonized maps generally had lower commission errors relative to the individual maps. The reduction in commission error of the harmonized maps was particularly dramatic for the 1986–1992 and 1992–2001 time intervals. For 2001–2006 and 2006–2011, the harmonized commission error rates were approximately the same as the commission error rates of the best of the individual maps. In general, commission errors were lower in the two more recent time periods compared with the earlier two time periods. The rules used to assign a label of “disturbed” in the harmonization process succeeded at reducing commission errors, but requiring two or more maps to agree on disturbance to produce a label of “disturbed” in the harmonized maps will result in the omission of some actual forest disturbance from the final harmonized maps.

To assess if high omission error rates were associated with the magnitude of disturbance, we characterized relative NBR change within sample plots by forest change type, categorizing disturbance magnitude for plots where harmonized maps match and omit forest disturbance. The mean NBR change for forest harvest/other mapped correctly in the harmonized maps was 12.0% (SE = 1.5%), while the mean NBR change for forest harvest/other disturbance omitted from the harmonized maps was 5.8% (SE = 0.9%). Clearly, omission errors of harvest/other disturbance were more likely to occur for lower magnitude events. For forest fire disturbance, the mean NBR change for forest fires mapped correctly in the harmonized maps was 20.4% (SE = 15.1%), while the mean NBR change for forest fires omitted from the harmonized maps was 14.5% (SE = 4.1%). Similar to harvest/other disturbances, the evidence indicates that fire disturbance omission errors occurred for lower magnitude fire events. The categorical comparison of NBR change for high (>66% relative change), medium (between 33 and 66% relative change), and low (<33% relative change) disturbances shows a high proportion of omitted plots characterized by low magnitude forest disturbance (89% for harvest/other and 76% for fire). However, matching plots also include many subtle forest changes and categorical differences are not significant.

Discussion

In the first time interval (1986–1992), only three datasets were available as surrogates for forest disturbance. Consequently, we were only able to include limited information in the harmonization process. In the harmonized 1986–1992 map, only 5% of the pixels selected in the final national forest disturbed map were labeled as forest disturbance by all input datasets. Heavy reliance on LF Raw VCT data during the harmonization procedure (Table 3) led to similar accuracy results between harmonized and stand-alone maps in 1986–1992, leading to no improvement in overall accuracy regarding the actual rate of disturbance. In 1992–2001, we included four datasets in the harmonization procedure and measured a noticeable increase in convergence between input data, where 34% of the pixels selected matched between three or more of the inputs. Overall accuracy improved in this interval relative to LF Raw VCT, thus resolving some uncertainty relative to previously published data. In the final two intervals (2001–2006 and 2006–2011), convergence between input data improved further, with 59 and 82% of the pixels retained in the final maps registering a match between three or more of the input datasets. Additionally, all stand-alone and harmonized forest disturbance maps had overall accuracy above 96%. While harmonized maps did not lead to greatly improved disturbance commission error rates (relative to the best single map) in the final two time intervals, the lower commission error rates in the last two time periods relative to the first two time periods for both harmonized and individual maps suggest that new generations of forest disturbance products are achieving improved disturbance mapping through advances in algorithm development and by increasing the temporal density of image stacks. By incorporating more images from the Landsat archive, new products are less likely to miss disturbance and more likely to converge on mapping reality more effectively.

Comparing the harmonized forest disturbance map accuracies against the individual forest disturbance maps indicated that harmonized maps had lower commission errors relative to individual maps in most intervals. However, harmonized maps had slightly higher omission errors in every interval. The conservative nature of the harmonization (i.e., requiring greater agreement among datasets) should yield lower commission error rates in the harmonized maps relative to the input datasets, but rejecting areas that do not agree between two or more datasets will increase omission errors by excluding some real forest disturbance from the final datasets.

The omission errors in stand-alone and harmonized maps illustrated that a considerable amount of forest disturbance was missed, but not all omission errors have identical impacts in end-user applications. Omission errors tended to be occur (on average) at lower magnitudes, and low magnitude disturbance is more common on a percent area basis. Landsat classification efforts do an effective job at mapping more destructive disturbances such as clear cuts and stand clearing forest fires but are currently limited in mapping subtle forest changes.

Harmonization consistently reduced commission errors compared with stand-alone forest disturbance map products. Reducing some of the noise associated with commission error may prove valuable to prospective end-users concerned about inflated forest disturbance estimates. The disturbance magnitude distribution reported here is also an informative way to conceptualize the limits to all forest disturbance mapping efforts. Subtle changes like forest thinning or sub-canopy fires may be omitted from current maps, yet these subtle changes are typically less destructive. Maps that encapsulate extreme forest disturbances provide a useful contribution to understanding changes that may have greater potential environmental impacts. Further, locations with cleared forest provide an opportunity to investigate stand regeneration lifecycles, from early-to-late successional cover.

Conclusions

Several forest disturbance products exist for CONUS and variability between forest these disturbance products leads to uncertainty regarding the actual rate and spatial distribution of disturbance. The goals of this study were to employ the concept of harmonization to create improved maps of forest disturbance, to conduct a rigorous accuracy assessment to quantify the relative difference in the harmonized maps compared with the individual input source products, and to augment the harmonized disturbance maps with information regarding the cause of the disturbance (fire versus harvest/other). After reconciling spatial, temporal, and definitional discrepancies between input data, we harmonized forest disturbances across four time intervals (1986–1992, 1992–2001, 2001–2006, and 2006–2011). While harmonization improved forest disturbance commission error rates relative to stand-alone maps, high disturbance omission error remained problematic. More complex algorithms for combining the input data to assign a label of "disturbed" may need to be developed to achieve the desired improvement in omission error rates. In the meantime, the harmonization procedure and relatively simple rule we applied to combine input map information provide improved commission error rates such that our harmonized maps will have value in identifying locations that have a high likelihood of disturbance. The documented map accuracy and the information regarding cause of disturbance will provide additional benefits to practitioners interested in using our harmonized maps.

Acknowledgments This research was supported by the USGS Land Change Science and USGS Climate Research and Development programs and Cooperative Agreement G12AC20221 provided by the USGS to SUNY ESF. We would also like to thank external peer reviewers for their suggestions. Any use of trade, firm, or product names is for descriptive purposes only and does not imply endorsement by the US Government.

References

Cohen, W. B., Spies, T. A., Alig, R. J., et al. (2002). Characterizing 23 years (1972-95) of stand replacement disturbance in Western Oregon forests with Landsat imagery. *Ecosystems, 5*, 122–137. doi:10.1007/s10021-001-0060-X.

Cohen, W. B., Yang, Z., & Kennedy, R. (2010). Detecting trends in forest disturbance and recovery using yearly Landsat time series: 2. TimeSync—tools for calibration and validation. *Remote Sensing of Environment, 114*, 2911–2924. doi:10.1016/j.rse.2010.07.010.

Cohen, W. B., Yang, Z., Stehman, S. V., et al. (2016). Forest disturbance across the conterminous United States from 1985–2012: the emerging dominance of forest decline. *Forest Ecology and Management, 360*, 242–252. doi:10.1016/j.foreco.2015.10.042.

Drobne, S., & Lisec, A. (2009). Multi-attribute decision analysis in GIS: weighted linear combination and ordered weighted averaging. *Informatica, 4*, 28.

Fensholt, R., Rasmussen, K., Nielsen, T. T., & Mbow, C. (2009). Evaluation of earth observation based long term vegetation trends—intercomparing NDVI time series trend analysis consistency of Sahel from AVHRR GIMMS, Terra MODIS and SPOT VGT data. *Remote Sensing of Environment, 113*, 1886–1898. doi:10.1016/j.rse.2009.04.004.

Finco, M., Quayle, B., Zhang, Y., et al. (2012). Monitoring trends and burn severity (MTBS): monitoring wildfire activity for the past quarter century using Landsat data. In: Moving from

Status to Trends: Forest Inventory and Analysis (FIA) Symposium. pp 222–228.

Friedl, M. A., Gray, J. M., Melaas, E. K., et al. (2014). A tale of two springs: using recent climate anomalies to characterize the sensitivity of temperate forest phenology to climate change. *Environmental Research Letters, 9*, 54006. doi:10.1088/1748-9326/9/5/054006.

Fry, J. A., Coan, M. J., Homer, C. G., et al. (2009). Completion of the National Land Cover Database (NLCD) 1992–2001 Land Cover Change Retrofit Product. U.S. Geological Survey, Open File Report 2008-1379.

Goetz, S. J., Fiske, G. J., & Bunn, A. G. (2006). Using satellite time-series data sets to analyze fire disturbance and forest recovery across Canada. *Remote Sensing of Environment, 101*, 352–365. doi:10.1016/j.rse.2006.01.011.

Goward, S. N., Masek, J. G., Cohen, W., et al. (2008). Forest disturbance and North American carbon flux. *EOS, Transactions, American Geophysical Union, 89*(11), 105–116.

Hansen, M. C., Egorov, A., Potapov, P. V., et al. (2014). Monitoring conterminous United States (CONUS) land cover change with Web-Enabled Landsat Data (WELD). *Remote Sensing of Environment, 140*, 466–484. doi:10.1016/j.rse.2013.08.014.

Hansen, M. C., Egorov, A., Roy, D. P., et al. (2011). Continuous fields of land cover for the conterminous United States using Landsat data: first results from the Web-Enabled Landsat Data (WELD) project. *Remote Sens Letters, 2*, 279–288. doi:10.1080/01431161.2010.519002 .

Hansen, M. C., Potapov, P. V., Moore, R., et al. (2013). High-resolution global maps of 21st-century forest cover change. *Science, 342*, 850–853. doi:10.1126/science.1244693.

Hansen, M. C., Stehman, S. V., & Potapov, P. V. (2010). Quantification of global gross forest cover loss. *Proceedings of the National Academy of Sciences, 107*, 8650–8655. doi:10.1073/pnas.0912668107.

Homer, C., Huang, C., Yang, L., et al. (2004). Development of a 2001 national land-cover database for the United States. *Photogrammetric Engineering and Remote Sensing, 70*, 829–840.

Houghton, R. A. (1999). The U.S. carbon budget: contributions from land-use change. *Science, 285*, 574–578. doi:10.1126/science.285.5427.574.

Huang, C., Goward, S. N., Masek, J. G., et al. (2010). An automated approach for reconstructing recent forest disturbance history using dense Landsat time series stacks. *Remote Sensing of Environment, 114*, 183–198. doi:10.1016/j.rse.2009.08.017.

Jansen, L. J. M. (2006). Harmonization of land use class sets to facilitate compatibility and comparability of data across space and time. *J Land Use Sci, 1*, 127–156. doi:10.1080/17474230601079241.

Jin, S., Yang, L., Danielson, P., et al. (2013). A comprehensive change detection method for updating the National Land Cover Database to circa 2011. *Remote Sensing of Environment, 132*, 159–175. doi:10.1016/j.rse.2013.01.012.

Jung, M., Henkel, K., Herold, M., & Churkina, G. (2006). Exploiting synergies of global land cover products for carbon cycle modeling. *Remote Sensing of Environment, 101*, 534–553. doi:10.1016/j.rse.2006.01.020.

Kennedy, R. E., Yang, Z., & Cohen, W. B. (2010). Detecting trends in forest disturbance and recovery using yearly Landsat time series: 1. LandTrendr—temporal segmentation algorithms. *Remote Sensing of Environment, 114*, 2897–2910. doi:10.1016/j.rse.2010.07.008.

Kennedy, R. E., Yang, Z., Cohen, W. B., et al. (2012). Spatial and temporal patterns of forest disturbance and regrowth within the area of the northwest forest plan. *Remote Sensing of Environment, 122*, 117–133. doi:10.1016/j.rse.2011.09.024.

Liski, J., Ilvesniemi, H., Mäkelä, A., & Starr, M. (1998). Model analysis of the effects of soil age, fires and harvesting on the carbon storage of boreal forest soils. *European Journal of Soil Science, 49*, 407–416. doi:10.1046/j.1365-2389.1998.4930407.x.

Loveland, T. R., Sohl, T. L., Stehman, S. V., et al. (2002). A strategy for estimating the rates of recent United States land cover changes. *Photogrammetric Engineering and Remote Sensing, 68*, 1091–1099.

Lunetta RS, Elvidge CD (1999) Remote sensing change detection: environmental monitoring methods and applications. Taylor & Francis Ltd

Lunetta, R. S., Knight, J. F., Ediriwickrema, J., et al. (2006). Land-cover change detection using multi-temporal MODIS NDVI data. *Remote Sensing of Environment, 105*, 142–154. doi:10.1016/j.rse.2006.06.018.

Masek, J. G., Goward, S. N., Kennedy, R. E., et al. (2013). United States forest disturbance trends observed using Landsat time series. *Ecosystems, 16*, 1087–1104. doi:10.1007/s10021-013-9669-9.

Moisen, G. G., & Frescino, T. S. (2002). Comparing five modelling techniques for predicting forest characteristics. *Ecological Modelling, 157*, 209–225.

Nelson, K. J., Connot, J., Peterson, B., & Martin, C. (2013). The Landfire refresh strategy: updating the national dataset. *Fire Ecology, 9*, 80–101. doi:10.4996/fireecology.0902080.

Olander, L. P., Gibbs, H. K., Steininger, M., et al. (2008). Reference scenarios for deforestation and forest degradation in support of REDD: a review of data and methods. *Environmental Research Letters, 3*, 25011.

Olofsson, P., Foody, G. M., Herold, M., et al. (2014). Good practices for estimating area and assessing accuracy of land change. *Remote Sensing of Environment, 148*, 42–57. doi:10.1016/j.rse.2014.02.015.

Omernik, J. M. (1987). Ecoregions of the conterminous United States. *Annals of the Association of American Geographers, 77*, 118–125. doi:10.1111/j.1467-8306.1987.tb00149.x .

Oswalt, S. N., Smith, W. B., Miles, P. D., et al. (2014). Forest resources of the United States, 2012; A technical document supporting the Forest Service 2015 update of the RPA Assessment: US Department of Agriculture, Forest Service, Washington Office. General Technical Report GTR–WO–91, p.218.

Pérez-Hoyos, A., García-Haro, F. J., & San-Miguel-Ayanz, J. (2012). A methodology to generate a synergetic land-cover map by fusion of different land-cover products. *International Journal of Applied Earth Observation and Geoinformation, 19*, 72–87. doi:10.1016/j.jag.2012.04.011 .

Rollins, M. G. (2009). LANDFIRE: a nationally consistent vegetation, wildland fire, and fuel assessment. *International Journal of Wildland Fire, 18*, 235. doi:10.1071/WF08088.

Roy, D. P., Ju, J., Kline, K., et al. (2010). Web-Enabled Landsat Data (WELD): Landsat ETM+ composited mosaics of the conterminous United States. *Remote Sensing of Environment, 114*, 35–49. doi:10.1016/j.rse.2009.08.011.

Särndal CE, Swensson B, Wretman J (1992) Model assisted survey sampling. Springer Science & Business Media

SAS/STAT Version 9.3. Statistical Analysis Software (SAS), Cary, North Carolina, USA

Schepaschenko, D., See, L., Lesiv, M., et al. (2015). Development of a global hybrid forest mask through the synergy of remote sensing, crowdsourcing and FAO statistics. *Remote Sensing of Environment, 162*, 208–220. doi:10.1016/j.rse.2015.02.011.

See, L. M., & Fritz, S. (2006). A method to compare and improve land cover datasets: application to the GLC-2000 and MODIS land cover products. *IEEE Transactions on Geoscience and Remote Sensing, 44*, 1740–1746. doi:10.1109/TGRS.2006.874750.

Song, X. P., Huang, C., Feng, M., et al. (2014). Integrating global land cover products for improved forest cover characterization: an application in North America. *International Journal of Digital Earth, 7*, 709–724. doi:10.1080/17538947.2013.856959.

Soulard, C. E., Acevedo, W., Auch, R. F., et al. (2014). Land Cover Trends Dataset, 1973–2000. *US Geological Survey doi*. doi:10.3133/ds844.

Vogelmann, J. E., Howard, S. M., Yang, L., et al. (2001). Completion of the 1990s National Land Cover Data Set for the conterminous United States from Landsat thematic mapper data and ancillary sources. *Photogrammetric Engineering and Remote Sensing, 67*, 650–662.

Vogelmann, J. E., Kost, J. R., Tolk, B., et al. (2011). Monitoring landscape change for LANDFIRE using multi-temporal satellite imagery and ancillary data. *IEEE Journal of Selected Topics in Applied Earth Observations and Remote Sensing, 4*, 252–264.

Wickham, J. D., Stehman, S. V., Gass, L., et al. (2013). Accuracy assessment of NLCD 2006 land cover and impervious surface. *Remote Sensing of Environment, 130*, 294–304. doi:10.1016/j.rse.2012.12.001.

Woodcock, C. E., Allen, R., Anderson, M., et al. (2008). Free access to Landsat imagery. *Science, 320*, 1011–1011. doi:10.1126/science.320.5879.1011a.

Woodcock, C. E., Macomber, S. A., Pax-Lenney, M., & Cohen, W. B. (2001). Monitoring large areas for forest change using Landsat: generalization across space, time and Landsat sensors. *Remote Sensing of Environment, 78*, 194–203.

Wulder, M. A., Masek, J. G., Cohen, W. B., et al. (2012). Opening the archive: How free data has enabled the science and monitoring promise of Landsat. *Remote Sensing of Environment, 122*, 2–10. doi:10.1016/j.rse.2012.01.010.

Xian, G., Homer, C., & Fry, J. (2009). Updating the 2001 National Land Cover Database land cover classification to 2006 by using Landsat imagery change detection methods. *Remote Sensing of Environment, 113*, 1133–1147. doi:10.1016/j.rse.2009.02.004.

Zhu, Z., & Woodcock, C. E. (2014). Continuous change detection and classification of land cover using all available Landsat data. *Remote Sensing of Environment, 144*, 152–171. doi:10.1016/j.rse.2014.01.011.

Zimmerman, P. L., Housman, I. W., Perry, C. H., et al. (2013). An accuracy assessment of forest disturbance mapping in the western Great Lakes. *Remote Sensing of Environment, 128*, 176–185.